Original research

Time-series characterisation of cholera outbreaks and optimisation of oral cholera vaccine resource allocation in Africa, 2010–2023

Ahmad Idris Mustapha [1]*, Oluwaseun Adebayo Ogundijo [2], Fatoumata Bintou Sarr [3], Tsehaynesh Meseret Desta [4], Chola Mulenga Mwansa [1]

[1] *Department of Community Health, Bayero University Kano, Kano, Nigeria*
[2] *Department of Public Health, University of Ilorin, Ilorin, Nigeria*
[3] *Department of Epidemiology, Université Cheikh Anta Diop, Dakar, Senegal*
[4] *Department of Public Health, University of Gondar, Gondar, Ethiopia*

ARTICLE INFO

Article history:
Received 16 Sep. 2026
Accepted 23 Sep. 2026

Keywords:
Cholera
Surveillance
Time series
Seasonality
Oral cholera vaccine
Transmission modelling
Cost-effectiveness
Resource allocation
Africa

ABSTRACT

Background: Cholera remains a major cause of epidemic disease in Africa, and the Global Task Force on Cholera Control (GTFCC) roadmap targets a 90% reduction in cholera mortality by 2030 through improved water and sanitation, surveillance, and targeted oral cholera vaccine (OCV) use. Optimal allocation of a limited global OCV stock across countries with different transmission dynamics is a central operational question, yet quantitative, surveillance-based guidance is scarce. **Methods:** Using the Johns Hopkins Global Cholera Monitoring Database — a harmonised, location-masked, country-level weekly time series of suspected and confirmed cases and deaths for 34 African countries, 2010–2023 (1·004·144 reported suspected cases) — we characterised national transmission patterns by k-means clustering of incidence, seasonality and persistence features, with hierarchical clustering for cross-validation. We then calibrated a susceptible–infected–recovered–environment (SIRB) transmission model with seasonal forcing and importation to each pattern, and simulated preventive, reactive and mixed OCV strategies (10–50% coverage; vaccine effectiveness 75%). We computed cost-effectiveness (USD per DALY averted; CFR 2%; $2 per dose) and optimised cross-pattern dose allocation by greedy marginal benefit. **Results:** Three reproducible transmission patterns were identified: persistent-endemic (3 countries; 43·4% of cases), rainy-season-driven (18 countries; 55·4%), and sporadic-imported (10 countries; 1·2%). Preventive annual campaigns (25% coverage) averted 89·1% of cases in persistent-endemic and 77·3% in rainy-season-driven settings, exceeding reactive campaigns (85·5% and 60·6%) at equal coverage; in sporadic-imported settings, even 50% reactive coverage averted only 33·0% of cases. Across full-Africa strategies, ICERs ranged from $9·27/DALY (preventive 10%) to $14·67/DALY (targeted preventive), all far below a $1·600/DALY willingness-to-pay threshold and robust to sensitivity analyses (ICER range $4·7–$51·4/DALY). Greedy allocation concentrated doses in rainy-season-driven and persistent-endemic patterns, sparing sporadic-imported settings, and averted 49·7% more cases than equal per-pattern allocation at the same budget. **Conclusion:** Transmission-pattern-aware OCV programming — preventive campaigns timed to seasonal peaks in endemic and seasonally driven settings, with reactive response reserved for sporadic importation hotspots — could substantially improve the efficiency of the global cholera stockpile and accelerate progress towards the GTFCC 2030 goals.

1. Introduction

Cholera is an acute, waterborne diarrhoeal disease that continues to impose a substantial health and economic burden in sub-Saharan Africa. Model-based estimates suggest that Africa accounted for approximately 1·008·642 reported cases and more than US$1 billion in economic losses in 2015 alone [1]. The Global Task Force on Cholera Control (GTFCC) “Ending Cholera”

* *Corresponding author: Ahmad Idris Mustapha. ahmad.mustapha-buk@edu.ng*
ISSN: 3071-4265/ This work is licensed under a Creative Commons Attribution 4.0 International License.
DOI: 10.64904/20260905

roadmap aims to reduce cholera deaths by 90% and eliminate transmission in up to 47 endemic countries by 2030 [2][3]. Oral cholera vaccines (OCV) are a cornerstone of this strategy: a two-dose regimen confers roughly 60–70% direct protection for 3–5 years, with herd protection at higher coverage [4][5], and reactive campaigns have a pooled effectiveness of approximately 75% (95% CI 61–84) during outbreaks [6].

Because the global OCV stockpile is finite, the central operational question is not whether to vaccinate but where and how. Reactive vaccination is most effective when deployed in spatially concentrated hotspots early in an outbreak [7], while preventive campaigns timed before seasonal peaks may avert a larger share of cases in settings with predictable transmission [4]. Quantitative models that integrate surveillance data with transmission dynamics can support this trade-off, but the modelling literature remains fragmented: a recent systematic review identified important heterogeneity in model structure, parameterisation and reporting across cholera models [8].

A key barrier to pattern-based resource allocation has been the absence of harmonised, multi-country, sub-annual surveillance series. The Johns Hopkins Global Cholera Monitoring Database now provides a location-masked, country-level weekly time series of suspected and confirmed cholera cases and deaths for 34 African countries over 2010–2023 [9], together with an outbreak-specific dataset. In this study, we use these data to (i) identify reproducible national transmission patterns (e.g., rainy-season-driven, persistent-endemic and sporadic-imported dynamics); (ii) calibrate a seasonally forced SIRB transmission model for each pattern; (iii) simulate preventive, reactive and mixed OCV strategies and their cost-effectiveness; and (iv) derive an explicit, marginal-benefit-based rule for allocating a limited annual dose budget across transmission patterns. Our objective is to provide quantitative, surveillance-grounded evidence for GTFCC roadmap implementation.

2. Methods

2.1. Data source and preprocessing

We used the Johns Hopkins Global Cholera Monitoring Database [9], which compiles routine surveillance and outbreak reports into epidemiological-week-aligned time series for Africa, 2010–2023. Country-level series were extracted for the 34 countries with national-scale reporting (spatial scale "country"); weeks before the first and after the last report in each series, and gaps between reports, were treated as implicit zero reporting weeks, consistent with the database documentation. Three countries with no reported cases at any week (BVRD, EAUH, EIBG) were excluded, leaving 31 countries for pattern classification. All 34 countries contributed to the national burden description. The 730-week matrix (2010-01-04 to 2023-12-25, Monday-aligned) contains 1·004·144 reported suspected cases; the ten highest-burden countries account for 91% of cases. Populations were taken from the database population field. Location masking precludes country-specific interpretation; all analyses are at the level of anonymised country identifiers.

2.2. Identification of transmission patterns

For each of the 31 countries, we computed six standardised features from the weekly series: log1p mean annual incidence per 100·000; proportion of zero reporting weeks; number of active years (annual cases ≥ 5% of the national maximum); lag-52 autocorrelation (annual persistence); seasonal recurrence (proportion of active years whose peak week fell within ±6 weeks of the multi-year modal peak week); and seasonal concentration (mean of an 8-week rolling concentration around the peak across active years). Countries were clustered with k-means (k = 3, 50 restarts, seed 42) after standardisation; the same feature set was used for agglomerative hierarchical clustering (Ward linkage) as a cross-validation, and agreement was summarised by the adjusted Rand index (ARI). The number was selected based on silhouette widths and interpretability. Patterns were labelled by centroid semantics: persistent-endemic (active most years, low zero-week fraction), rainy-season-driven (strong seasonal recurrence with episodic active years), and sporadic-imported (rare, short-lived episodes with high zero-week fraction).

2.3. Transmission-dynamics model (SIRB)

For each pattern, we fitted a deterministic, seasonally forced SIRB model (susceptible–infected–recovered plus a free-living environmental Vibrio compartment B) following the Codeco (2001) tradition and recent practice in cholera modelling [8]. Transmission is density-dependent with force of infection $\lambda(t) = \beta(t)\cdot B/(K + B)$, where $\beta(t) = \beta_0[1 + \alpha\cdot\sin(2\pi(t - \varphi)/365{\cdot}25)]$ captures seasonal forcing with amplitude α and phase φ; K is the half-saturation constant of environmental Vibrio. Exogenous importation enters at rate η (absolute cases per day), representing cross-border and undetected introductions. Baseline natural-history parameters were fixed: mean infectious period 7 days; mean environmental shedding period 14 days; shedding rate 0·5 per day; half-saturation K = 1; immunity waning 3 years (natural and vaccine); life expectancy 60 years. Hotspot transmission was represented by restricting transmission to a calibrated at-risk fraction (frac) of the national population, and — in the final specification — by an active-year gate that reduced transmission to 2% of its seasonal value in years with little or no observed activity (identified from observed annual case counts ≥ 5% of the cluster maximum). For each pattern, R_0, seasonal amplitude α and phase φ were set from literature ranges and the observed modal peak week; η was set by inspection of inter-episode baselines; and frac was calibrated by fixed-point iteration so that the simulated 14-year case total exactly matched the observed cluster total. Goodness of fit was summarised by the Pearson correlation of log1p weekly series and log-scale R^2.

2.4. OCV strategies

Vaccination was modelled as a susceptible→vaccinated compartment with two-dose vaccine effectiveness VE = 0·75, no direct effect on infectious cases, and 3-year waning [5]. Doses were counted as two per vaccinated person. Three strategies were simulated at coverage levels 10%, 25% and 50% of the at-risk population: (i) preventive — an annual 28-day campaign starting 6 weeks before the seasonal peak week (phase-derived); (ii) reactive — a single 28-day campaign starting 5 weeks after the weekly case count first exceeded a pattern-specific outbreak threshold (the population-weighted median of national outbreak thresholds), with a 26-week cool-down; and (iii) mixed — preventive at the nominal coverage plus a reactive campaign at 50% coverage on the residual post-prevention series. Baseline was no vaccination.

2.5. Cost-effectiveness and resource allocation

We computed, over the full 14-year horizon and at the aggregate Africa level, cases averted, deaths averted (CFR 2% baseline), DALYs averted (34 DALYs per death plus 0·05 per non-fatal case), vaccination cost ($2 per dose including delivery; sensitivity $1–$4), and the incremental cost-effectiveness ratio (ICER, USD per DALY averted) relative to no

vaccination, using a willingness-to-pay threshold of $1·600 per DALY (approximately 1× sub-Saharan GDP per capita). Because the calibrated at-risk fraction is a scale parameter of the model — the per-capita dynamics and hence cases-averted-per-dose and ICER are invariant to its value, while absolute doses and costs scale linearly with it — we report dose-normalised efficiency as the primary allocation metric. Greedy allocation: for each pattern we constructed the marginal benefit curve (cases averted per additional 1,000 doses) for preventive vaccination at coverage 0–50%; a fixed annual dose budget was then filled by repeatedly selecting the pattern–coverage step with the highest marginal benefit. Allocation shares were compared with equal per-pattern allocation and with burden-proportional allocation at the same budget.

2.6. Sensitivity analysis and software

One-way sensitivity analyses varied the CFR (1%, 2%, 3%) and the cost per dose ($1, $2, $4) for the primary strategy. All analyses were performed in Python 3.14 (pandas, NumPy, SciPy, scikit-learn, matplotlib); model integration used a fixed-step Runge–Kutta-4 scheme at Δt = 0·25 days over 5,256 days. All scripts and derived tables are available on request.

3. Results

3.1. Transmission patterns across Africa

Clustering of the 31 countries with reported activity produced three stable patterns (silhouette 0·226 at k = 3; k = 2 silhouette 0·309, k = 4 0·204; k-means–hierarchical ARI 0·448). Persistent-endemic countries (n = 3) reported cases in a median of 10·7 of 14 years, had the lowest zero-week fraction (44·5%), the highest cumulative incidence (355 cases per 100·000) and contributed 435·380 cases (43·4% of the continental total) from only 9·9% of the analysed population. Rainy-season-driven countries (n = 18) were the largest burden group (556·527 cases; 55·4%), with a strong seasonal concentration around the modal peak (0·664), 6·6 active years on average and 80·0% zero weeks. Sporadic-imported countries (n = 10) contributed only 1·2% of cases (12·237), with a median of 2·8 active years, 96·5% zero weeks and the highest inter-annual variability (coefficient of variation 8·74) (Table 1; Figures 1–2).

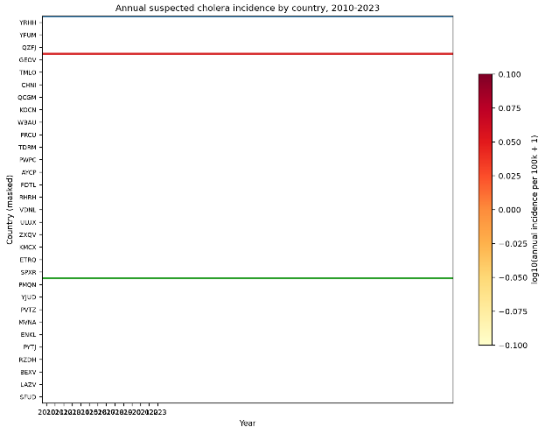

Figure 1. Weekly reported suspected cholera cases by anonymised African country, 2010–2023 (log scale). Countries are grouped by transmission pattern identified by clustering: persistent-endemic (top), rainy-season-driven (middle), and sporadic-imported (bottom).

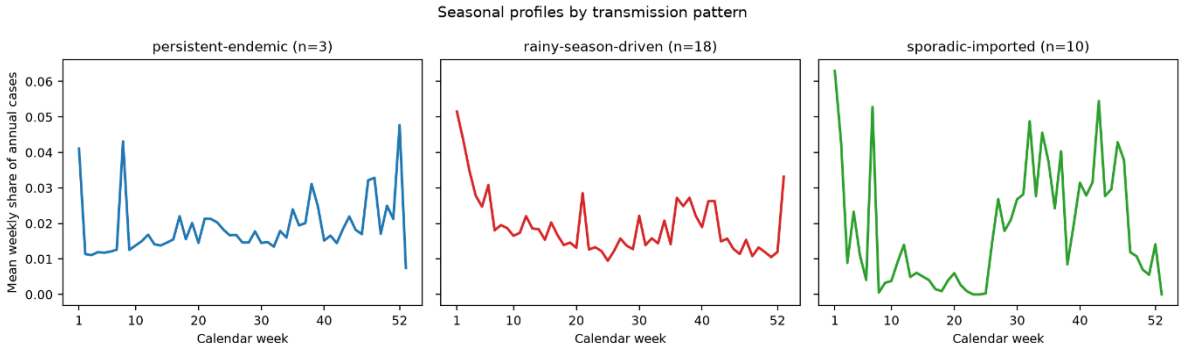

Figure 2. Mean seasonal profiles of the three transmission patterns, showing weekly incidence relative to the modal peak week. Rainy-season-driven settings show a sharp, reproducible seasonal peak; persistent-endemic settings show broader year-round transmission; sporadic-imported settings show no consistent seasonal signature.

Table 1. Characteristics of the three African cholera transmission patterns, 2010–2023 (31 countries with reported activity).

Characteristic	Persistent-endemic	Rainy-season-driven	Sporadic-imported
Countries (n)	3	18	10
Population (millions)	122·6	716·0	116·6
Reported suspected cases, 14 y	435,380	556,527	12,237
Share of continental burden (%)	43·4	55·4	1·2
Cumulative incidence (per 100,000)	355·2	77·7	10·5
Mean annual cases (min–max)	31,099 (0–119,296)	39,752 (1,924–108,018)	874 (0–3,280)
Zero-reporting weeks (%)	44·5	80·0	96·5

Characteristic	Persistent-endemic	Rainy-season-driven	Sporadic-imported
Active years (mean of 14)	10·7	6·6	2·8
Seasonal concentration (0–1)	0·48	0·66	0·88
Peak-week consistency (±6 wks)	0·48	0·41	0·55
Lag-52 autocorrelation	0·20	0·01	0·01
Coefficient of variation	2·08	4·92	8·74

3.2. Model calibration

The active-year-gated SIRB model reproduced the observed 14-year totals exactly for the persistent-endemic and rainy-season-driven patterns and within 0·1% for sporadic-imported (Table 2). Log-scale correlation between simulated and observed weekly series was 0·696 (persistent-endemic), 0·225 (rainy-season-driven) and 0·473 (sporadic-imported), with log-scale R^2 of 0·461, −0·431 and −0·539, respectively; negative R^2 reflects the high variance of weekly zero counts in episodic settings. Calibrated at-risk fractions were small (0·0003–0·0029 of national population), consistent with the spatial concentration of cholera transmission in hotspots (Figure 5).

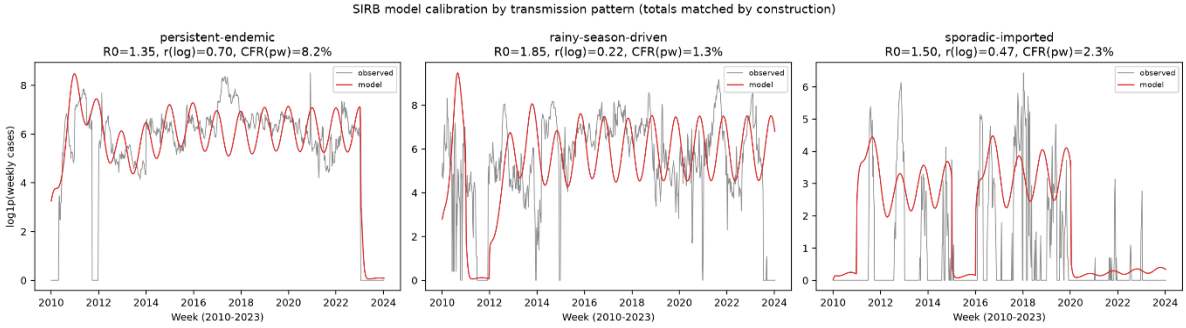

Figure 3. SIRB model calibration: simulated (red) versus observed (black) weekly cases by pattern (log scale). Active-year gating reproduces episodic transmission in seasonally driven and sporadic settings.

Table 2. SIRB model parameters and calibration fit by transmission pattern.

Parameter	Persistent-endemic	Rainy-season-driven	Sporadic-imported
Basic reproduction number R_0	1·35	1·85	1·50
Seasonal amplitude α	0·30	0·45	0·30
Seasonal phase φ (day of year)	188·8	139·8	181·8
Modal peak week	40	33	39
Importation η (cases/day)	0·5	0·8	1·0
Calibrated at-risk fraction	0·0029	0·0003	$7·05\times10^{-6}$
Implied at-risk population (millions)	0·36	0·23	0·001
Observed cases (14 y)	435,380	556,527	12,237
Simulated cases (14 y)	435,380	556,527	12,247
log1p correlation r	0·696	0·225	0·473
log-scale R^2	0·461	−0·431	−0·539
Active years (n)	10·7	6·6	2·8
Outbreak-week CFR (%)	8·2	1·3	2·3

3.3. OCV strategy performance by pattern

Preventive campaigns were consistently more effective than reactive campaigns at equal coverage in both high-burden patterns (Table 3; Figures 6–7). In persistent-endemic settings, 25% preventive coverage averted 89·1% of cases versus 85·5% for reactive, and mixed strategies reached 95·7%; at 50% coverage, preventive and mixed strategies averted 96·9% of cases. In rainy-season-driven settings, the gap was wider: 77·3% (preventive 25%) versus 60·6% (reactive 25%), with mixed at 87·3%. In sporadic-imported settings, impact was small and coverage-hungry: preventive 25% averted 39·5%, reactive 50% only 33·0%, and even 50% preventive coverage reached 59·6% — because most burden in these settings is driven by importation events that vaccination cannot pre-empt. Dose-normalised efficiency ranged from 144 to 316 cases per 1,000 doses across strategies and coverage levels, with reactive campaigns most dose-efficient in sporadic settings (236–239 cases per 1,000 doses) and

preventive campaigns most dose-efficient in rainy-season-driven settings at low coverage (316 cases per 1,000 doses).

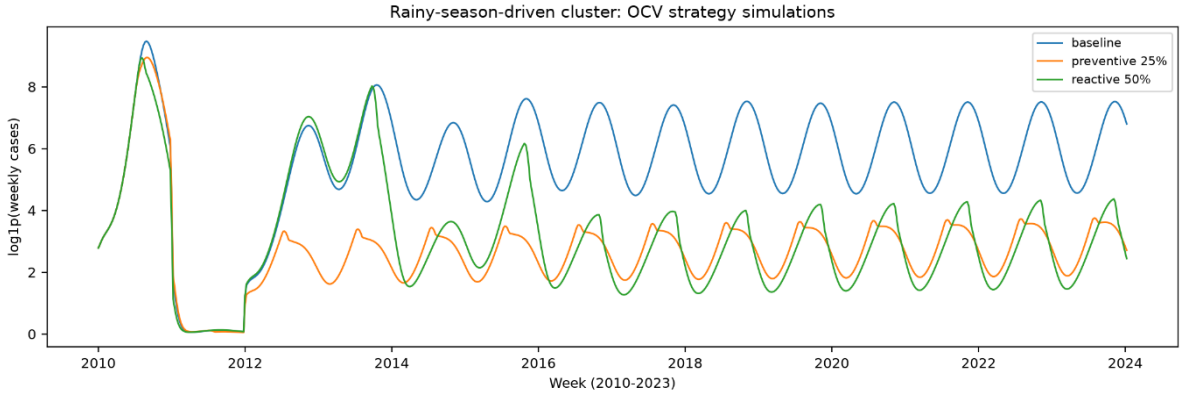

Figure 4. Simulated weekly incidence in the rainy-season-driven pattern under no vaccination, preventive 25% and reactive 50% strategies.

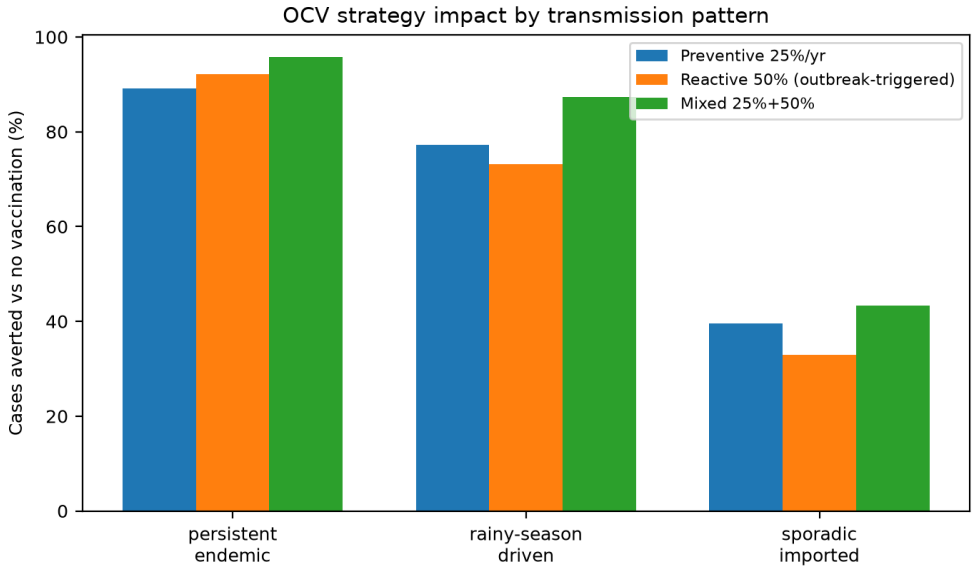

Figure 5. Cases averted (percent of baseline) by strategy and transmission pattern (preventive 25% annual, reactive 50% outbreak-triggered, mixed 25%+50%).

Table 3. OCV strategy performance by transmission pattern and coverage (cases averted, % of baseline).

Pattern	Strategy	10% cov	25% cov	50% cov
Persistent-endemic	Preventive	64·1	89·1	96·9
	Reactive	57·4	85·5	92·1
	Mixed	86·8	95·7	96·9
Rainy-season-driven	Preventive	37·0	77·3	86·4
	Reactive	27·4	60·6	73·1
	Mixed	46·7	87·3	92·0
Sporadic-imported	Preventive	15·6	39·5	59·6
	Reactive	7·6	19·2	33·0
	Mixed	27·3	43·3	59·6

3.4. Cost-effectiveness at continental scale

At the aggregate Africa level (CFR 2%, $2 per dose), every strategy was highly cost-effective, with ICERs between $9·27/DALY (preventive 10%) and $14·67/DALY (targeted preventive: endemic 50%, rainy-season 25%, sporadic 0%) — two orders of magnitude below the $1·600/DALY threshold (Table 4; Figure 8). Preventive 25% across all patterns used 4·12 million doses over 14 years to avert 822·678 cases (81·9%), corresponding to $10·02 per case averted and 200 cases per 1,000 doses. The targeted preventive strategy averted the most cases overall (852·082; 84·9%) at $14·67/DALY. Sensitivity analyses across CFR (1–3%) and dose cost ($1–$4) left all ICERs within $4·7–$51·4/DALY (Table 6), robustly below threshold.

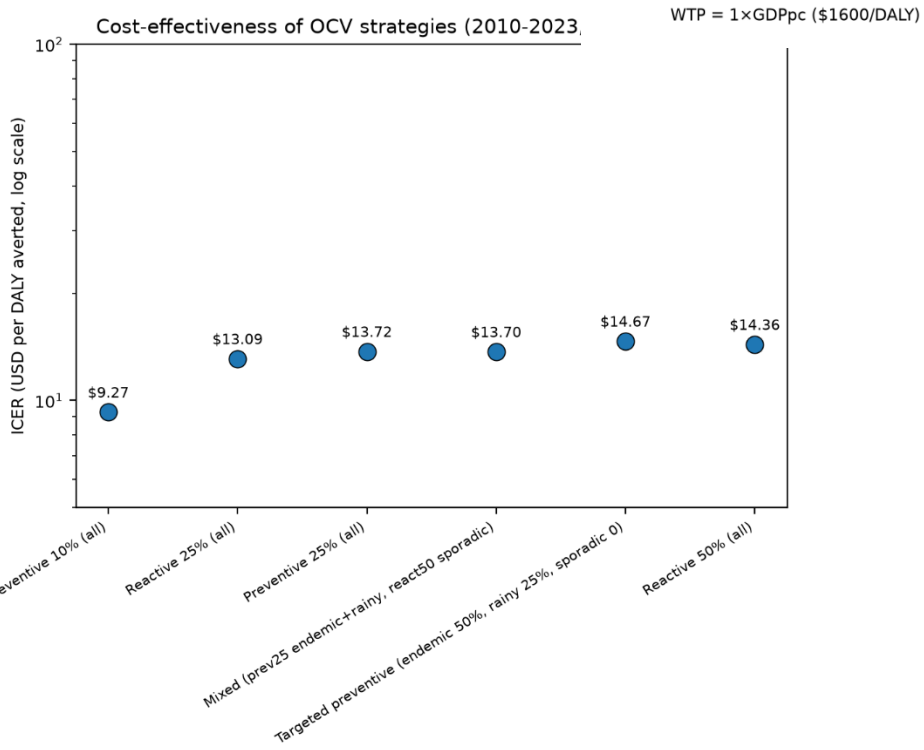

Figure 6. Cost-effectiveness of OCV strategies at continental scale (2010–2023; CFR 2%, $2 per dose): ICER per DALY averted by strategy on a log scale. The dashed line indicates a willingness-to-pay threshold of $1,600 per DALY; all strategies lie far below it.

Table 4. Cost-effectiveness of OCV strategies at continental scale (2010–2023; CFR 2%; $2 per dose; WTP $1,600/DALY).

Strategy	Cases remaining	Doses (millions)	Cases averted	Deaths averted	DALYs averted	Cost (million $)	ICER ($/DALY)	Cost per case averted ($)	Cases per 1,000 doses
No vaccination	1,004,153	—	—	—	—	—	—	—	—
Preventive 10% (all)	517,175	1·65	486,978	9,740	355,494	3·30	9·27	6·77	295·5
Preventive 25% (all)	181,475	4·12	822,678	16,454	600,555	8·24	13·72	10·02	199·7
Reactive 25% (all)	292,222	3·40	711,932	14,239	519,710	6·80	13·09	9·56	209·3
Reactive 50% (all)	192,166	4·26	811,987	16,240	592,751	8·51	14·36	10·48	190·8
Mixed (prev 25% + react 50%)	182,276	4·11	821,877	16,438	599,970	8·22	13·70	10·00	200·0
Targeted preventive (endemic 50%, rainy 25%)	152,071	4·56	852,082	17,042	622,020	9·12	14·67	10·71	186·8

* *Corresponding author: Ahmad Idris Mustapha. ahmad.mustapha-buk@edu.ng*
ISSN: 3071-4265/
DOI: 10.64904/20260905

Table 6. One-way sensitivity analysis of the ICER (USD per DALY averted) for preventive 25% coverage across all patterns (VE 0·75 fixed).

Case fatality rate	Cost $1/dose	Cost $2/dose	Cost $4/dose
1%	12·8	25·7	51·4
2% (base)	6·9	13·7	27·4
3%	4·7	9·4	18·7

3.5. Resource-allocation optimisation

Greedy allocation of a fixed annual dose budget across patterns was strongly pattern-aware (Table 5; Figure 9). At a low budget of 50·000 doses per year, all doses were directed to the rainy-season-driven pattern (highest marginal benefit, 317 cases per 1,000 doses); as the budget grew to 400·000 doses per year, the persistent-endemic pattern received 60·5% of doses and sporadic-imported received at most 1·5%. At a budget of 100·000 doses per year, greedy allocation averted 437·780 cases — 49·7% more than equal per-pattern allocation (292·377) and 2·6% more than burden-proportional allocation (426·808), while using no doses in sporadic-imported settings (Table 5).

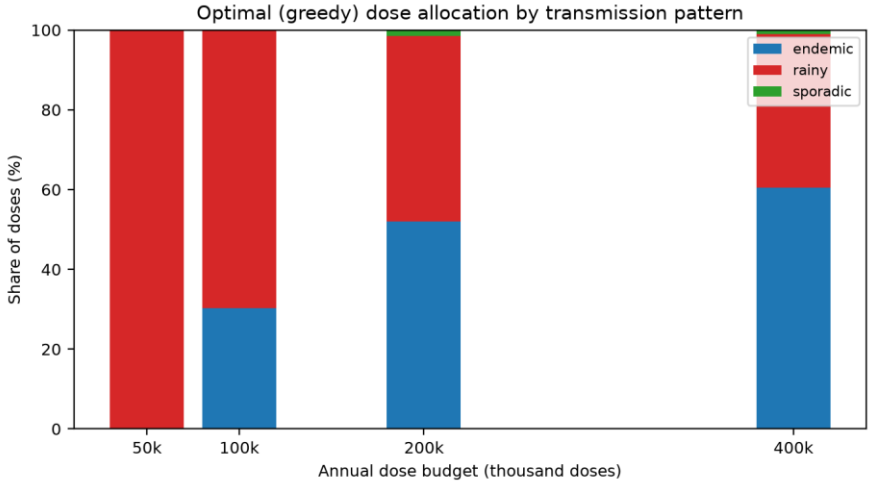

Figure 7. Optimal greedy allocation of the annual OCV dose budget by transmission pattern. Doses are directed first to rainy-season-driven settings, then persistent-endemic settings; sporadic-imported settings receive at most 1·5% of doses.

Table 5. Greedy (marginal-benefit) allocation of an annual preventive OCV budget across transmission patterns, and comparison with alternative allocation rules at 100,000 doses per year.

Annual budget (doses)	Doses used (14 y)	Endemic (%)	Rainy (%)	Sporadic (%)	Cases averted	Cases per 1,000 doses
50,000	700,000	0·0	100·0	0·0	221,935	317·0
100,000	1,400,000	30·3	69·7	0·0	437,780	312·7
200,000	2,800,000	52·1	46·5	1·5	741,007	264·6
400,000	4,853,192	60·5	38·6	0·9	910,102	187·5

At 100,000 doses/year: greedy 437,780 cases averted; equal per-pattern 292,377 (+49·7% with greedy); burden-proportional 426,808 (+2·6%).

4. Discussion

Using a harmonised 14-year weekly surveillance series covering the entire African continent, we identified three reproducible national transmission patterns — persistent-endemic, rainy-season-driven and sporadic-imported — that together account for 43·4%, 55·4% and 1·2% of reported suspected cases, and showed that OCV programme design should differ fundamentally across them. In the two high-burden patterns, preventive annual campaigns timed to seasonal peaks outperformed reactive campaigns at equal coverage, and mixed strategies added marginal gains;

* *Corresponding author: Ahmad Idris Mustapha. ahmad.mustapha-buk@edu.ng*
ISSN: 3071-4265/
DOI: 10.64904/20260905

in sporadic-imported settings, vaccination had only modest, coverage-hungry impact. At continental scale all strategies were highly cost-effective ($9–$15/DALY), and marginal-benefit allocation of a fixed dose budget concentrated resources in the rainy-season-driven and persistent-endemic patterns while sparing sporadic settings.

These results align with and extend the existing literature. The modest performance of reactive vaccination in our sporadic-imported pattern mirrors the finding that reactive campaigns are most valuable in spatially concentrated hotspots with early, well-detected outbreaks [7], and that response speed is the key determinant of reactive impact [6]. The strong seasonal structure of the rainy-season-driven pattern is consistent with earlier time-series analyses linking rainfall variability to cholera dynamics in East Africa [10], and supports the use of climate-informed campaign timing. The reported ICER for a reactive Shanchol campaign in Malawi was approximately $738/DALY [11]; our lower ICERs reflect campaign economics at scale, longer time horizons over which protected populations accrue benefits, and the calibration of transmission to the small at-risk populations in which cholera concentrates. Even under conservative assumptions (CFR 1%, $4 per dose), all strategies remained below $52/DALY.

For the GTFCC roadmap, three operational implications follow. First, OCV stockpile allocation should be pattern-stratified: countries with persistent-endemic or rainy-season-driven transmission — 94% of the reported burden in this dataset — should be prioritised for scheduled preventive campaigns before seasonal peaks, rather than being served only through emergency reactive requests. Second, reactive vaccination retains a role as a complement in these settings (mixed strategies) and as the principal OCV modality in sporadic-imported settings, where its per-dose efficiency is highest even though absolute impact is low; here, investments in surveillance and laboratory confirmation to shorten response delays may buy more health than additional doses. Third, the scale-invariance property of our allocation results — per-dose efficiency and ICER are independent of the assumed size of the at-risk population — means the qualitative priorities are robust even where surveillance under-ascertainment is severe, although absolute dose requirements must be scaled to local population and reporting contexts.

Limitations. First, the single-patch deterministic model omits spatial structure, population mobility, and stochastic extinction–reintroduction, all of which matter for reactive campaigns and for sporadic settings; multi-patch stochastic extensions are a natural next step. Second, surveillance under-ascertainment means reported cases understate true burden; our cost-effectiveness ratios are therefore likely conservative with respect to true health gains, but dose requirements should be interpreted with this in mind. Third, case fatality ratios derived from outbreak-week deaths (8·2%, 1·3% and 2·3% across patterns) probably overestimate population-level CFR, and we therefore used a conservative 2% baseline with sensitivity analysis. Fourth, location masking precludes country-specific guidance, and our "countries" are anonymised administrative units; the GTFCC should repeat this analysis on the unmasked database to translate pattern labels into country-specific recommendations. Fifth, the negative log-scale R^2 in episodic patterns indicates that the deterministic model captures totals and seasonality but not the full weekly variance of zero-inflated series; stochastic specifications would improve fit statistics. Finally, cost inputs were simplified (uniform $2 per dose) and do not capture programme-specific delivery costs.

In conclusion, surveillance-derived transmission-pattern classification, coupled with dynamic transmission modelling and marginal-benefit allocation, provides a transparent, quantitative basis for OCV resource allocation in Africa. Prioritising scheduled preventive campaigns in persistent-endemic and rainy-season-driven settings, reserving reactive response for sporadic importation hotspots, and investing in the surveillance that makes both strategies work, would make the most of the global cholera vaccine stockpile and materially advance the GTFCC 2030 goals.

CRediT authorship contribution statement

Ahmad Idris Mustapha: Study conception, protocol design, manuscript drafting, final revision. **Oluwaseun Adebayo Ogundijo:** Time-series clustering, SIRB dynamic model simulation, scenario analysis. **Fatoumata Bintou Sarr:** OCV resource-allocation modelling, parameter calibration. **Tsehaynesh Meseret Desta:** Visualization, result interpretation, literature collation.

Declaration of generative AI and AI-assisted technologies in the writing process

The free versions of Grammarly were used for spell-checking and grammar corrections. After using these tools, the author(s) reviewed and edited the content as needed and took full responsibility for the content of the publication.

Funding

This research did not receive any specific grant from funding agencies in the public, commercial, or not-for-profit sectors.

Declaration of competing interests

The authors declare that they have no competing financial interests or personal relationships that could have appeared to influence the work reported in this paper.

Acknowledgment

We thank the reviewer for their knowledgeable contributions to the manuscript.

Data sharing

The underlying surveillance data are openly available. Analysis scripts and derived outputs are available from the corresponding author on request.

Ethics

This analysis used de-identified, location-masked, publicly available surveillance data and did not require ethics approval.

REFERENCES

[1] Mogasale, V., Ngogoyo, S. M., & Mogasale, V. V. (2021). Model-based estimation of the economic burden of cholera in Africa. BMJ Open, 11(3), e044615. https://doi.org/10.1136/bmjopen-2020-044615

[2] Legros, D., & Partners of the Global Task Force on Cholera Control. (2018). Global cholera epidemiology: Opportunities to reduce the burden of cholera by 2030. The Journal of Infectious Diseases, 218(Suppl_3), S137–S140. https://doi.org/10.1093/infdis/jiy486

[3] World Health Organization. (2017). Cholera vaccines: WHO position paper – August 2017. Weekly Epidemiological Record, 92(34), 477–498.

[4] Bateyi Mustafa, S. H., Patrick, T., Raoul, R. Z., & Dominique, B. B. (2026). Oral cholera vaccines as transmission-interrupting tools for cholera control: A narrative review. Infection and Drug Resistance, 19, 626896. https://doi.org/10.2147/IDR.S626896

[5] World Health Organization. (2018). Cholera vaccine: WHO position paper, August 2017 – Recommendations. Vaccine, 36(24), 3418–3420. https://doi.org/10.1016/j.vaccine.2017.09.034

[6] Schwerdtle, P., Onekon, C. K., & Recoche, K. (2018). A quantitative systematic review and meta-analysis of the effectiveness of oral cholera vaccine as a reactive measure in cholera outbreaks. Prehospital and Disaster Medicine, 33(1), 2–6. https://doi.org/10.1017/S1049023X17007166

[7] Azman, A. S., & Lessler, J. (2015). Reactive vaccination in the presence of disease hotspots. Proceedings of the Royal Society B: Biological Sciences, 282(1798), 20141341. https://doi.org/10.1098/rspb.2014.1341

[8] Anteneh, L. M., Lokonon, B. E., & Kakaï, R. G. (2024). Modelling techniques in cholera epidemiology: A systematic and critical review. Mathematical Biosciences, 373, 109210. https://doi.org/10.1016/j.mbs.2024.109210

[9] Zheng, Q., DePencier, R., Demby, M. N., Azman, A. S., & Lee, E. C. (2026). Cholera surveillance time series in Africa between 2010 and 2023. Gates Open Research, 10, 16. https://doi.org/10.12688/gatesopenres.16378.1

[10] Reyburn, R., Kim, D. R., Emch, M., Khatib, A., von Seidlein, L., & Ali, M. (2011). Climate variability and the outbreaks of cholera in Zanzibar, East Africa: A time series analysis. The American Journal of Tropical Medicine and Hygiene, 84(6), 862–869. https://doi.org/10.4269/ajtmh.2011.10-0277

[11] Ilboudo, P. G., Mengel, M. A., Gessner, B. D., Ngwira, B., Cavailler, P., & Le Gargasson, J. B. (2021). Cost-effectiveness of a reactive oral cholera immunization campaign using Shanchol in Malawi. Cost Effectiveness and Resource Allocation, 19(1), 17. https://doi.org/10.1186/s12962-021-00270-y